Doping evolution of itinerant magnetic fluctuations in Fe-based pnictides

A Letters Journal Exploring the Frontiers of Physics

September 2008

EPL, **83** (2008) 67003
doi: 10.1209/0295-5075/83/67003

www.epljournal.org

Doping evolution of itinerant magnetic fluctuations in Fe-based pnictides

M. M. Korshunov[1,2(a)] and I. Eremin[1,3(b)]

[1] *Max-Planck-Institut für Physik Komplexer Systeme - 01187 Dresden, Germany, EU*
[2] *L.V. Kirensky Institute of Physics, Siberian Branch of Russian Academy of Sciences - 660036 Krasnoyarsk, Russia*
[3] *Institute für Mathematische und Theoretische Physik, TU-Braunschweig - 38106 Braunschweig, Germany, EU*

received 20 May 2008; accepted in final form 24 July 2008
published online 8 September 2008

PACS 74.20.-z – Theories and models of superconducting state
PACS 74.25.Ha – Magnetic properties
PACS 75.30.Fv – Spin-density waves

Abstract – Employing the four-band tight-binding model, we study theoretically the doping dependence of the spin response in the normal state of novel Fe-based pnictide superconductors. We show that the commensurate spin density wave (SDW) transition that arises due to interband scattering between the hole α-pockets and the electron β-pockets disappears already at the doping concentration $x \approx 0.04$ reflecting the evolution of the Fermi surfaces. Correspondingly, with further increase of the doping the antiferromagnetic fluctuations are suppressed for $x > 0.1$ and the imaginary part of the spin susceptibility at antiferromagnetic wave vector becomes nearly temperature independent. At the same time, we observe that the uniform susceptibility deviates from the Pauli-like behavior and is increasing with increasing temperature reflecting the activation processes for the α-Fermi surfaces up to temperatures of about $T = 800\,\mathrm{K}$. With increase of the doping the absolute value of the uniform susceptibility lowers and its temperature dependence changes. In particular, it is a constant at low temperatures and then decreases with increasing temperature. We discuss our results in a context of recent experimental data.

Introduction. – The recent discovery of superconductivity in the iron-based layered superconductor $La(O_{1-x}F_xFeAs)$ with $T_c \approx 26\,\mathrm{K}$ [1] has generated a renewed interest in high-temperature superconductivity due to consequent development of materials with higher T_c's up to 55 K that contain other rare-earth elements such as Ce, Nd, Sm [2–4] instead of La. The physical properties are considered to be highly two-dimensional; the crystal structure is tetragonal and consists of the LaO and the FeAs layers which are stacked along the c-axis. Similar to many layered transition metal oxides the superconductivity in oxypnictides occurs upon introducing doping of either electrons [1–4] or holes [5] into the FeAs layers and the parent material shows antiferromagnetic transition at around 150 K [1,6–9]. At the same time, in contrast to layered cuprates the parent material remains a metal. The observed magnetic moment per Fe atom has been reported to range between $0.25\mu_B$ [9] and $0.36\mu_B$ [7] and lies in the ab-plane.

There have been various proposals to explain the origin of antiferromagnetism in these systems. Recent theoretical studies suggest several different explanations varying from LaOFeAs being an antiferromagnetic semimetal [10–12], or a system with frustrated magnetic ground state with two interpenetrating antiferromagnetic square sublattices [13–16]. However, the resulting magnetic moment is larger than that found in experiment thus requiring an inclusion of strong fluctuations effects that would reduce the magnetic moment. At the same time, starting from purely itinerant models it has been also proposed that LaOFeAs has an antiferromagnetic spin density wave instability due to the interband nesting of the electron and the hole Fermi surfaces [6,9,17]. The resulting magnetic moment has been found to be about $0.33\,\mu_B$ which agrees with experimental data. Despite the right order of magnitude it remains to be seen whether the strong electronic correlations that might be important in LaOFeAs due to Hund's exchange [18,19] will modify this result. It has

(a) E-mail: maxim@pks.mpg.de
(b) On leave from Kazan State University - 420008 Kazan, Russian Federeation; E-mail: ieremin@pks.mpg.de

been also argued that a combined effect of spin-orbit coupling, monoclinic distortions, and p-d hybridization may invalidate the simple Hund's coupling scheme [20].

In order to understand how the magnetism and the spin fluctuations in $La(O_{1-x}F_xFeAs)$ evolve as a function of doping in this letter we present the study of magnetic excitations using the tight-binding scheme adopted previously [21]. In particular, we show that the commensurate spin density wave (SDW) transition that arises due to interband scattering between the hole α-pockets and the electron β-pockets at the Fermi surface (FS) disappears already at the doping concentration $x \approx 0.04$. Correspondingly, with further increase of the doping the antiferromagnetic fluctuations are suppressed and at $x \approx 0.1$ the $\mathrm{Im}\chi(\mathbf{Q}_{AFM}, \omega)/\omega$ becomes nearly temperature independent. At the same time, we observe the uniform susceptibility deviates from the Pauli-like behavior and increases with increasing temperature reflecting the activation processes for the α-Fermi surfaces up to temperatures of about 800 K. With increase of the doping the absolute value of the uniform susceptibility decreases and its temperature dependence changes. It is a constant at low temperatures and then decreases with increasing temperature.

Theory. – The effective low-energy band structure of the undoped LaOFeAs can be modeled by the following single-electron model Hamiltonian for the folded Brillouin Zone (BZ) with two Fe-ions per unit cell [21]:

$$H_0 = -\sum_{\mathbf{k},\alpha,\sigma} \epsilon^i n_{\mathbf{k}i\sigma} - \sum_{\mathbf{k},i,\sigma} t^i_{\mathbf{k}} d^\dagger_{\mathbf{k}i\sigma} d_{\mathbf{k}i\sigma}, \qquad (1)$$

where $i = \alpha_1, \alpha_2, \beta_1, \beta_2$ refer to the band indices, ϵ^i are the on-site single-electron energies, $t^{\alpha_1,\alpha_2}_{\mathbf{k}} = t^{\alpha_1,\alpha_2}_1(\cos k_x + \cos k_y) + t^{\alpha_1,\alpha_2}_2 \cos k_x \cos k_y$ is the electronic dispersion that yields hole α-pockets centered around the Γ-point, and $t^{\beta_1,\beta_2}_{\mathbf{k}} = t^{\beta_1,\beta_2}_1(\cos k_x + \cos k_y) + t^{\beta_1,\beta_2}_2 \cos\frac{k_x}{2}\cos\frac{k_y}{2}$ is the dispersion that results in the electron β-pockets around the M-point of the folded BZ. Using the abbreviation $(\epsilon^i, t^i_1, t^i_2)$ we choose the parameters $(-0.60, 0.30, 0.24)$ and $(-0.40, 0.20, 0.24)$ for the α_1 and α_2 bands, respectively, and $(1.70, 1.14, 0.74)$ and $(1.70, 1.14, -0.64)$ for the β_1 and β_2 bands, correspondingly (all values are in eV).

In fig. 1(a) we show the resulting energy dispersion along the main symmetry directions of the first BZ for the undoped case, $x = 0$. The band structure parameters were chosen to correctly reproduce the LDA Fermi surface topology and the values of the Fermi velocities for the hole α- and the electron β-pockets. In particular, we have selected the on-site energies and the hopping matrix elements assuming the compensated metal at $x = 0$ and calculating the chemical potential self-consistently for the filling factor $n = 4$ (we further assume that there exists another band below the Fermi level which is fully occupied and not considered here). As a consequence, the hole Fermi surfaces shifted by vector (π, π) is nearly completely nested with that of the electron pockets in full agreement

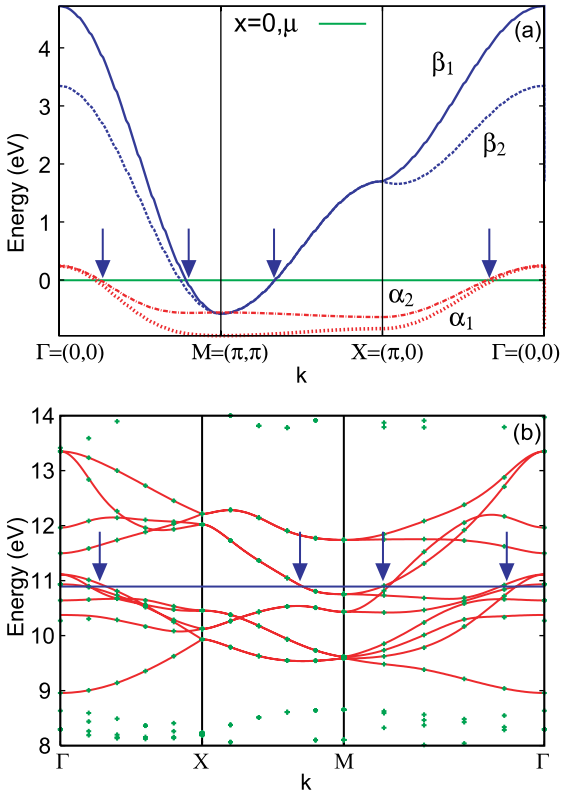

Fig. 1: (Colour on-line) (a) Calculated energy dispersion along the main symmetry points of the first BZ for the undoped, $x = 0$, case. (b) LDA band structure (green crosses) and ten-band model dispersion (red curves) after Kuroki *et al.* [23]. Note the difference in BZ directions in (a) and (b). The large arrows indicate the points where bands cross the Fermi level.

with *ab initio* density functional calculations [6,18,22,23]. Additionally, we take into account the details of the electronic dispersions of the bands forming the Fermi surface pockets. In order to visualize the comparison, in fig. 1(b) we present the LDA band structure and the realistic ten-band model dispersion from ref. [23]. Note, for other doping concentrations the position of the chemical potential was deduced from the equation $n = 4 + x$.

The resulting doping-dependence of the physical susceptibility as obtained by the sum of all interband and intraband susceptibilities is shown in fig. 2. For the undoped case our results are in qualitative agreement with that of Kuroki *et al.* [23] and Raghu *et al.* [24], and with the *ab initio* results of Dong *et al.* [6].

Within the random phase approximation (RPA) the spin response has a matrix form:

$$\hat{\chi}_{RPA}(\mathbf{q}, \mathrm{i}\omega_m) = [\mathbf{I} - \mathbf{\Gamma}\hat{\chi}_0(\mathbf{q}, \mathrm{i}\omega_m)]^{-1}\hat{\chi}_0(\mathbf{q}, \mathrm{i}\omega_m), \qquad (2)$$

where $\mathbf{I}$ is a unit matrix and $\hat{\chi}_0(\mathbf{q}, \mathrm{i}\omega_m)$ is 4×4 matrix formed by the interband and the intraband bare susceptibilities. For the four-band model considered here the effective interaction consist of the on-site Hubbard intraband repulsion U and Hund's coupling J. There is also

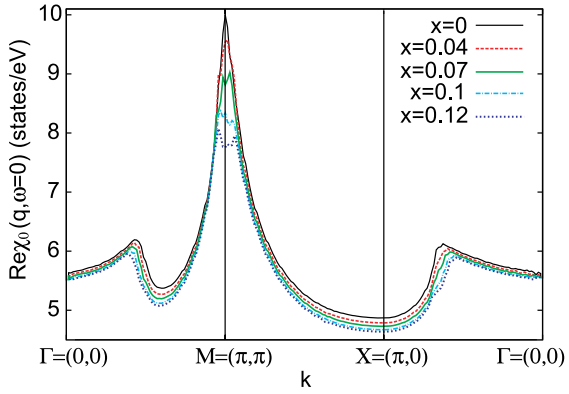

Fig. 2: Calculated doping dependence of the real part of the physical spin susceptibility, $\chi_0(\mathbf{q},0)=\sum_{ij}\chi_0^{ij}(\mathbf{q},0)$, where i,j refer to the band index.

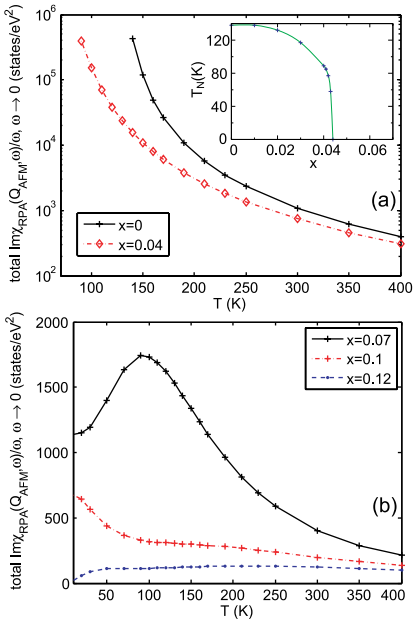

Fig. 3: Calculated $\lim_{\omega\to 0}\mathrm{Im}\chi_{RPA}(\mathbf{Q}_{AFM},\omega)/\omega$ for various doping concentrations. Note the log scale in (a). The inset in (a) shows the calculated doping dependence of the Néel transition temperature.

an interband Hubbard repulsion U', which, however, does not contribute to the RPA spin susceptibility. The vertex is given by

$$\mathbf{\Gamma}=\begin{bmatrix} U & J/2 & J/2 & J/2 \\ J/2 & U & J/2 & J/2 \\ J/2 & J/2 & U & J/2 \\ J/2 & J/2 & J/2 & U \end{bmatrix}. \tag{3}$$

For the given Fermi surface topology the main magnetic instability in the folded BZ occurs at the antiferromagnetic wave vector $\mathbf{Q}_{AFM}=(\pi,\pi)$ due to the interband nesting between the hole α- and the electron β-bands [6,21,22,24]. This is also clearly visible from our fig. 2. Note that in the unfolded BZ with one Fe-ion per unit cell, the wave vector is $\mathbf{Q}'_{AFM}=(\pi,0)$ which corresponds to the "stripe"-like ordering of the Fe-spins as observed by neutron scattering [7]. Setting Hund's coupling to $J=70\,\mathrm{meV}$ and choosing $U=320\,\mathrm{meV}$, we obtain the ordering temperature $T_N=138\,\mathrm{K}$ as determined by $\det[\mathbf{I}-\mathbf{\Gamma}\hat{\chi}_0(\mathbf{q},\mathrm{i}\omega_m)]=0$. Solving the condition for the SDW instability below T_N which can be regarded as a mean-field equation for the SDW order parameter, we obtain $\Delta_{SDW}(T=0\,\mathrm{K})=31\,\mathrm{meV}$ which corresponds to the magnetic moment per two Fe sites to be $\mu\approx 0.33\,\mu_B$.

Note, the small values of U and J used here are a consequence of the absence of self-energy corrections within the RPA approach. Such corrections would reduce the value of the absolute magnitude of the spin susceptibility and correspondingly yield larger values of the coupling constants U and J.

In the inset of fig. 3(a) we show the doping dependence of the Néel temperature. One finds that it decreases quite rapidly as a function of doping and goes to zero already at $x\approx 0.04$. The reason for the rapid suppression of the Néel temperature is quite obvious. Away from $x=0$ the spectral weight of the hole α-pockets at the Fermi surface decreases and the condition for interband nesting becomes worse as is readily seen from fig. 2. In particular, one finds that the peak at the antiferromagnetic wave vector, $\mathbf{Q}_{AFM}$, decreases quite rapidly away from $x=0$. It is remarkable that such a small deviation from the undoped case changes the situation dramatically also in the NMR experimental data [25] that gives an additional support in favor of the nesting scenario of the antiferromagnetic transition.

In fig. 3 we show the doping-dependent evolution of the $\lim_{\omega\to 0}\mathrm{Im}\chi(\mathbf{Q}_{AFM},\omega)/\omega$. One finds that at $x=0$ it diverges at T_N and with further increase of the doping the antiferromagnetic fluctuations are quickly suppressed. Remarkably one finds that $\mathrm{Im}\chi(\mathbf{Q}_{AFM},\omega)/\omega$ at $x=0.12$ does not show any enhancement characteristic for strong antiferromagnetic spin fluctuations and stays nearly constant. Despite the fact that the real part still shows peaks around $\mathbf{Q}_{AFM}$, the antiferromagnetic fluctuations are quite strongly suppressed in the imaginary part of the spin susceptibility. This is due to the fact that the RPA response has a matrix form and thus the damping of the fluctuations is quite strong. At the same time, one has to keep in mind that the spin dynamics on the As sites originating from the stripe-like ordering of the Fe spins as probed by NMR may be suppressed due to hyperfine interaction. Therefore, further experimental studies are necessary to understand the evolution of the antiferromagnetic fluctuations in these systems.

In fig. 4 we show the temperature dependence of the uniform susceptibility for various doping concentrations. It is interesting to note that the uniform susceptibility above T_N does not show either Pauli-like or Curie-Weiss–type behavior. At zero doping concentration the total susceptibility increases as a function of temperature up to 600 K and then decreases following a Curie-Weiss–like

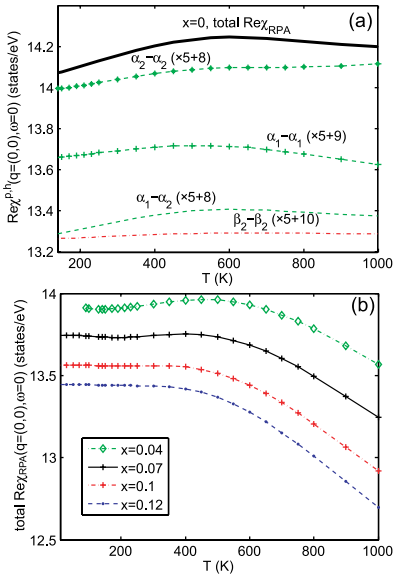

Fig. 4: Calculated uniform part of the total spin susceptibility, $\chi_{RPA}(\mathbf{q}\to 0,\omega\to 0)$ as a function of temperature at $x=0$ (a) and for other doping concentrations (b). In (a) we show also the partial contributions including the interband and the intraband transitions.

behavior. Looking at the partial contributions, one finds that this temperature dependence is determined mainly by the transitions between α-bands which produce the hole pockets around the Γ-point in the BZ. In particular, the hole-like Fermi surfaces of the α_1 and α_2 bands are only slightly splitted. The gap between the two Fermi energies that would occur for zero *transferred* momentum is about 50 meV. Therefore, due to the temperature activated transitions between two α bands, the interband susceptibility will increase with increasing temperature up to 600 K and then decrease. This slight increase of susceptibility is quantitatively consistent with the available experimental measurements [9,26]. Note that the transitions within β bands and between α and β bands show almost Pauli-like behavior. Upon changing doping, the overall magnitude of the susceptibility decreases which reflects the reduction of the total susceptibility as also shown in fig. 2. The latter occurs due to the filling of the hole pockets. We also observe the change in the temperature dependence of the uniform susceptibility. For $x>0.1$ the uniform susceptibility is constant up to 200 K and then decreases with increasing temperature. This change occurs due to the filling of the α-bands upon varying doping and the reduction of their relative splitting as can be seen from fig. 1.

We finally note that in our analysis we assume all matrix elements for the calculations of the spin susceptibility to be unity. A qualitative agreement between our results and those found in refs. [6,23,24] for the undoped case seems to justify our approach. In addition we further neglect the other three-dimensional band that gets quickly filled upon doping. Although its inclusion may be important with regard to the formation of three-dimensional Néel order, it will not change much the doping dependence of the two-dimensional in-plane magnetic fluctuations.

Conclusion. – We have analyzed the doping dependence of the spin excitations in $La(O_{1-x}F_x)FeAs$ based on a purely itinerant model. We find that the interband antiferromagnetic spin fluctuations are rather rapidly suppressed and the Néel temperature disappears already for $x\approx 0.04$. With further increase of the doping the short-range antiferromagnetic fluctuations disappear at $x\approx 0.12$ in agreement with NMR data. Given the fact that the superconductivity seems to be strongest at this doping concentration, it is interesting to see whether these fluctuations can be responsible for the formation of superconductivity. Due to the multi-orbital character, the uniform susceptibility shows neither Pauli-like nor Curie-like behavior. In particular, for low doping the total susceptibility increases up to 600 K and then decreases. With increasing doping the susceptibility stays constant at small temperatures and then lowers with increasing temperatures. We find that this characteristic behavior originates from the interband transitions between slightly splitted α-bands.

Note added: After submission of this manuscript we became aware of the study by Anisimov *et al.* [27], where the values of the average Coulomb repulsion U and Hund's exchange J were obtained by the first-principles constrained density functional theory in Wannier functions formalism. Due to the delocalization of Wannier functions for the Fe-3d basis set, the Coulomb parameters were significantly reduced in comparison to their intra-atomic values and became $U\approx 0.6$ eV and $J\approx 0.5$ eV. These are close to the effective parameters used in the present study.

* * *

We would like to thank B. Büchner, S.-L. Drechsler, D. Efremov, P. Fulde, I. Mazin, R. Moessner and D. Parker for useful discussions. IE acknowledges support from Volkswagen Foundation.

REFERENCES

[1] Kamihara Y., Watanabe T., Hirano M. and Hosono H., *J. Am. Chem. Soc.*, **130** (2008) 3926.
[2] Chen X. H., Wu T., Wu G., Liu R. H., Chen H. and Fang D. F., *Nature*, **453** (2008) 761.
[3] Chen G. F. *et al.*, *Phys. Rev. Lett.*, **100** (2008) 247002.
[4] Ren Z.-A. *et al.*, *Mater. Res. Innov.*, **12** (2008) 1.
[5] Wen H. H., Mu G., Fang L., Yang H. and Zhu X., *Europhys. Lett.*, **82** (2008) 17009.
[6] Dong J. *et al.*, *Europhys. Lett.*, **83** (2008) 27006.
[7] de la Cruz C. *et al.*, *Nature*, **453** (2008) 899.
[8] Nomura T. *et al.*, arXiv:0804.3569 (2008).
[9] Klauss H. H. *et al.*, *Phys. Rev. Lett.*, **101** (2008) 077005.

[10] Cao C., Hirschfeld P. J. and Cheng H.-P., *Phys. Rev. B*, **77** (2008) 220506(R).
[11] Ma F. and Lu Z.-Y., *Phys. Rev. B*, **78** (2008) 033111.
[12] Yin Z. P., Lebègue S., Han M. J., Neal B., Savrasov S. Y. and Pickett W. E., *Phys. Rev. Lett.*, **101** (2008) 047001.
[13] Yildirim T., *Phys. Rev. Lett.*, **101** (2008) 057010.
[14] Fang C., Yao H., Tsai W.-F., Hu J. and Kivelson S. A., *Phys. Rev. B*, **77** (2008) 224509.
[15] Ma F., Lu Z.-Y. and Xiang T., arXiv:0804.3370 (2008).
[16] Xu C., Mueller M. and Sachdev S., *Phys. Rev. B*, **78** (2008) 020501(R).
[17] Han Q., Chen Y. and Wang Z. D., *Europhys. Lett.*, **82** (2008) 37007.
[18] Haule K., Shim J. H. and Kotliar G., *Phys. Rev. Lett.*, **100** (2008) 226402.
[19] Haule K. and Kotliar G., arXiv:0805.0722 (2008).
[20] Wu J., Phillips Ph. and Castro-Neto A. H., arXiv:0805.2167 (2008).
[21] Korshunov M. M. and Eremin I., arXiv:0804.1793 (2008).
[22] Mazin I. I., Singh D. J., Johannes M. D. and Du M. H., *Phys. Rev. Lett.*, **101** (2008) 057003.
[23] Kuroki K., Onari S., Arita R., Usui H., Tanaka Y., Kontani H. and Aoki H., *Phys. Rev. Lett.*, **101** (2008) 087004.
[24] Raghu S., Qi X.-L., Liu C.-X., Scalapino D. and Zhang S.-C., *Phys. Rev. B*, **77** (2008) 220503(R).
[25] Nakai Y., Ishida K., Kamihara Y., Hirano M. and Hosono H., *J. Phys. Soc. Jpn.*, **77** (2008) 073701.
[26] Klingeler R. *et al.*, arXiv:0808.0708 (2008).
[27] Anisimov V. I. *et al.*, arXiv:0807.0547 (2008).